Journal of Power Sources 185 (2008) 871–875

Contents lists available at ScienceDirect

Journal of Power Sources

journal homepage: www.elsevier.com/locate/jpowsour

Short communication

Synthesis and characterization of nanostructured PtCo-CeO_x/C for oxygen reduction reaction

Kang Hee Lee, Kyungjung Kwon*, Victor Roev, Duck Young Yoo, Hyuk Chang, Doyoung Seung

Energy & Environment Lab, Samsung Advanced Institute of Technology, Nongseo-dong, Giheung-gu, Yongin-si, Gyeonggi-do 446-712, Republic of Korea

ARTICLE INFO

Article history:
Received 16 May 2008
Received in revised form 28 July 2008
Accepted 2 September 2008
Available online 19 September 2008

Keywords:
Electrocatalyst
Polymer electrolyte membrane fuel cell
Oxygen reduction
Platinum
Cerium
Platinum–cobalt alloy

ABSTRACT

Highly dispersed PtCo–CeO_x couples of fine Pt_3Co alloy particles with adjacent CeO_x are synthesized on a carbon support using the modified colloid method. The average sizes of Pt_3Co and CeO_x particles are approximately 1.7 and 4 nm, respectively. According to XPS studies, the CeO_x particle consists of a CeO_2 phase crystal for the core and a Ce_2O_3 phase for the shell. The CeO_x-containing electrocatalysts of PtCo–CeO_x and Pt–CeO_x show improved electrochemical performances for the oxygen reduction reaction compared with PtCo and Pt electrocatalysts without CeO_x in both ring-disc electrode and cell tests. It seems that the unsaturated Ce_2O_3 phase of the CeO_x surface causes the facile adsorption and desorption of oxygen, leading to an enhanced oxygen supply to the PtCo alloy.

1. Introduction

Polymer electrolyte membrane fuel cells (PEMFCs) have attracted much interest because of their extended application in various fields such as mobile power sources and residential power systems [1]. One of the major obstacles that should be overcome for the commercialization of PEMFCs is to find a more efficient catalyst than Pt for the oxygen reduction reaction (ORR), which is the cathodic reaction of a PEMFC.

Platinum alloyed with Co, Fe, Ni, Cr or V has received much scientific attention as the cathode catalyst because of its superior ORR activity to pure Pt [2–6]. The improvement in the ORR has been ascribed to modifications of the geometric and electronic structures, as well as the Pt–Pt bond distance and d-electron vacancy, by alloying with the transition metals [7]. In fact the modifications could affect the bond strength between Pt alloy and surface oxygen. The kinetics of the ORR is determined by the number of free Pt sites available for the adsorption of oxygen. The fractional coverage by OH occupied on Pt alloys is related to their d-band centre position. In a recent study on this electronic effect [8], PtCo alloy having an appropriate energy level of the metal d-band shows a better ORR activity, which is attributed to its lower OH coverage in the ORR.

The supply rate of oxygen is another significant factor that could affect the kinetics of the ORR. The high overpotential in the cathode of hydrogen-based PEMFCs could be overcome through rapid oxygen transfer to the Pt catalyst. Additions of Sn, Mo and W to the oxide phase in fuel cell electrodes have been studied to facilitate the supply of oxygen species leading to improved cell performance [9,10]. CeO_2, a widely used rare earth metal oxide catalyst, is efficient for the control of automotive emissions because of its ability of oxygen storage [11]. CeO_2 has also been used as an electrolyte material because of the high oxygen transfer ability derived from its own oxygen defects [12]. It has been reported [13–18] that CeO_2 promotes CO oxidation in the anode of direct alcohol fuel cells by supplying oxygen ions to the Pt catalyst. Although the oxygen supply problem more critically affects the fuel cell performance on cathode compared with anode, the application of CeO_2 for the ORR is described only in a few studies [19,20]. As a promising design for cerium-containing electrocatalyst for the ORR, we tried to combine optimally designed cerium oxide with a PtCo alloy, which is one of the most effective ORR catalysts [21]. In this study, PtCo alloy–CeO_x is prepared by a modified colloid method. Although this method has already been adopted [22] to prepare PtRu alloy for a direct methanol fuel cell (DMFC) anode catalyst, the fabrica-

* Corresponding author. Tel.: +82 31 280 8162; fax: +82 31 280 9359.
E-mail address: k.kwon@samsung.com (K. Kwon).

0378-7753/$ – see front matter © 2008 Elsevier B.V. All rights reserved.
doi:10.1016/j.jpowsour.2008.09.029

tion of metal–metal oxide couples on carbon in this study is a new initiative.

2. Experimental

A total of 5 g of $NaHSO_3$ was added to 200 g of a 1 M solution of hydrated platinum chloride ($H_2PtCl_6{\cdot}xH_2O$) as a platinum precursor dissolved in water, and thoroughly stirred to produce a solution of $H_2Pt(SO_3)_2Cl_6{\cdot}OH$. A total of 50 ml of hydrogen peroxide was added to the solution to produce PtO_2. Then, 0.5 g of $CoCl_2{\cdot}6H_2O$ as a cobalt precursor and 0.5 g of $(NH_4)_2Ce(NO_3)_6$ as a cerium precursor were added and reacted with the hydrogen peroxide that had remained in the solution, to produce cobalt oxide (CoO_x) and cerium oxide (CeO_x). To the colloid solution, 0.5 g of Ketchen black was added as a carbon catalytic support while bubbling in hydrogen, and stirring was performed for a further 12 h. The filtered solid product was washed several times with water and then dried under a nitrogen atmosphere at 120 °C. The resulting solid product was thermally reduced at 280 °C in hydrogen gas to produce the electrocatalyst for fuel cells.

The surface of the final electrocatalyst product was analyzed using a transmission electron microscope (TEM). Meanwhile, the final product was analyzed by means of X-ray photoemission spectroscopy (XPS).

The electrochemical properties of the catalyst were evaluated with a rotating disc electrode (RDE) system (Princeton Applied Research Bistat & Ring-disc Electrode System). Glassy carbon was used as the substrate for the working electrode and catalyst ink was made according to the method of Schmidt et al. [23]. Aqueous suspension of catalyst, dispersed via ultrasonification, was pipetted on to the glass carbon substrate. After evaporation of the water droplet, Nafion solution (0.05 wt.%, Aldrich) was applied on top of the dried catalyst powder. The RDE experiments were performed with a half cell in which the reference electrode was Ag|AgCl and the counter electrode was platinum foil. The electrolyte was a 0.5 M H_3PO_4 aqueous solution. Cyclic voltammetry was conducted with the nitrogen-saturated electrolyte at a scan rate of 10 mVs^{-1}, and linear scan voltammetry for the ORR evaluation was performed with an oxygen-saturated electrolyte at a scan rate of 1 mVs^{-1}. The potentials throughout this study are reported with respect to the reversible hydrogen electrode (RHE).

A polybenzoxazine-based membrane was used for the membrane electrode assembly (MEA) evaluation of catalysts, and the amount of phosphoric acid in the membrane was controlled by immersing a dry membrane in phosphoric acid at 80 °C for a few hours [24]. The cathode catalyst layer was composed of PtCo–CeO_x or PtCo supported on Ketzen black and polyvinylidene fluoride (PVDF). The anode catalyst layer was a carbon-supported PtRu alloy from Tanaka Kikinzoku Kogyo and PVDF. The Pt loadings of the cathode and anode were approximately 1.6 and 1.0 mg cm^{-2}, respectively. Dry hydrogen for the anode and dry air for the cathode were used for cell operation that was conducted at 150 °C. The effective dimensions of the electrode in the MEA were 2.8 cm × 2.8 cm.

3. Results and discussion

A schematic diagram of the novel catalyst design is shown in Fig. 1. The design concept of this catalyst system consists of two main ideas. One is that the PtCo alloy should contact with CeO_x that transfers oxygen ions in the PtCo–CeO_x unit. The oxygen ions would be adsorbed on Ce^{III} sites that have an unsaturated coordination of oxygen species, would be released to the PtCo alloy while the oxidation state of Ce is reversibly changed from 4+ to 3+. The other idea of the design is that CeO_x should exist in the size of nanoparticles. More effective ORR would occur on the alloy–oxide interfaces where a rapid oxygen supply is possible when compared with the PtCo alloy alone. The procedure involving an aqueous oxidation of Pt, Co and Ce by H_2O_2 and an aqueous reduction of Pt and Co by hydrogen gas was applied to the simultaneous formation of PtCo alloy and cerium oxide. A gaseous reduction procedure was finally performed for the complete reduction of PtCo and the removal of Cl residuals. The same synthesis procedure was applied to Pt/C, PtCo/C and Pt–CeO_x/C for comparison with PtCo–CeO_x/C.

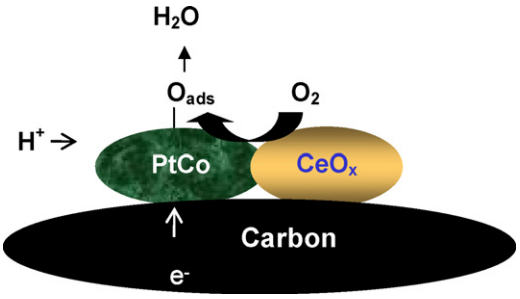

Fig. 1. Design of PtCo–CeO_x/C catalyst for ORR.

As shown in Table 1, the loading of Pt catalysts prepared by the colloid method is 40 wt.%, as determined by inductively coupled plasma (ICP) analysis. The amount of Co and Ce are approximately 4 and 6 wt.% on a total catalyst weight basis including the carbon support, respectively. The controlled Co amount results in the formation of Pt_3Co crystals, which are known to be the most active PtCo composition for the ORR. Since CeO_x has a low electrical conductivity, an appropriate quantity will be required so as not to depress significantly the conductivity of the catalysts for cell performance. Catalysts containing various amounts of CeO_x are prepared and tested for the ORR activity. The optimum content of CeO_x will be discussed in the remainder of this article with respect to electrochemical data.

The TEM photographs of PtCo/C, Pt–CeO_x/C and PtCo–CeO_x/C are shown in Fig. 2. The particle size and distribution of the PtCo alloys on carbon were studied to confirm the feasibility of the modified colloid method. It can be seen that PtCo nanoparticles are well distributed on the carbon support and their average particle size is 1.73 nm. In an additional X-ray diffraction (XRD) analysis, the PtCo alloy particles do not show any peaks on the XRD pattern due to their undetectable size. It is also found that CeO_x is closely combined with Pt in both Pt–CeO_x/C and PtCo–CeO_x/C catalysts with the size of the CeO_x nanoparticles being approximately 4 nm also. Various independent PtCo particles are also present due to the lower content of cerium compared with the amount of Pt. The crystal phases of PtCo and CeO_x are identified as Pt_3Co and CeO_2 by lattice analysis, as can be seen from the nanoparticles with lattice spacing 0.222 and 0.313 nm corresponding to Pt_3Co[1 1 1] and CeO_2[1 1 1], respectively [25].

The regional XPS spectrums of cerium and platinum in PtCo–CeO_x/C are presented in Fig. 3. In the samples, well-resolved

Table 1
Bulk compositions and electrochemical performances of prepared catalysts for ORR.

Catalyst	Composition[a] (wt.%)	ESA[b] ($m^2\ g^{-1}$)	Mass activity for ORR ($A\ g^{-1}$)
Pt/C	Pt 35.2	22.1	6.8
PtCo/C	Pt 39.6/Co 3.2	29.9	7.6
Pt–CeO_x/C	Pt 35.3/Ce 6.0	21.6	8.5
PtCo–CeO_x/C	Pt 39.6/Co 4.1/Ce 6.2	30.7	9.3

[a] Obtained from ICP analysis.
[b] Electrochemical surface area.

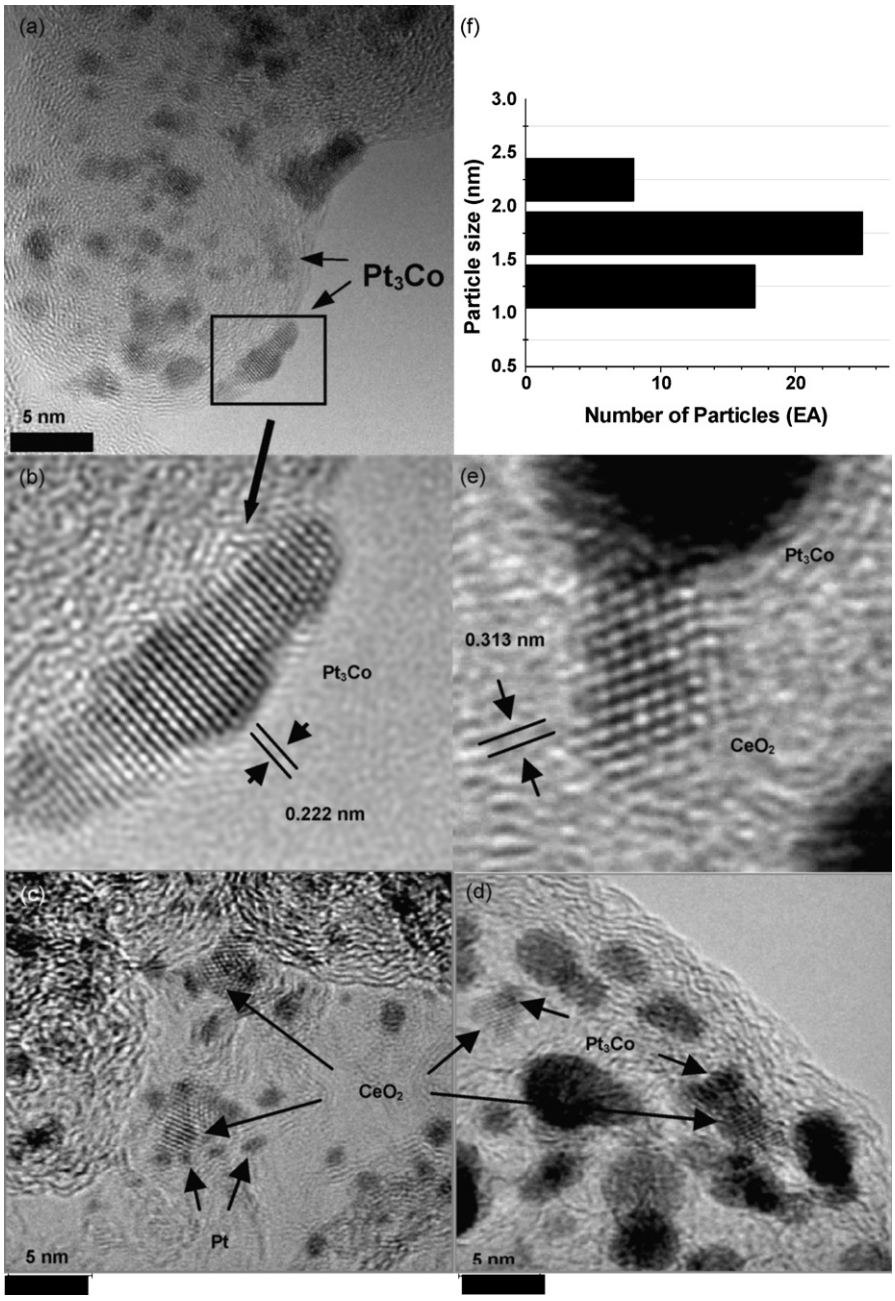

Fig. 2. Transmission electron microscope images of prepared catalysts and the particle-size distribution of PtCo alloy: (a) and (b) PtCo/C; lattice spacing d of 0.22 nm corresponding to [1 1 1] lattice fringe of Pt_3Co crystal, (c) Pt–CeO_x/C, (d) PtCo–CeO_x/C and (e) PtCo–CeO_x/C; lattice spacing d of 0.313 nm corresponding to [1 1 1] lattice fringe of CeO_2 crystal; (f) particle-size distribution of PtCo particles from PtCo/C.

components of Ce 3d are observed. XPS analysis is used to determine the oxidation states of cerium oxide and the Pt species. The 3d Ce region can be deconvoluted into peaks at 886.6 and 904.7 eV derived from the 3+ oxidation state and peaks at 882.9 and 901.3 eV from the 4+ oxidation state [26]. The dominant Ce state is 3+ as evident from the size of the corresponding peaks. It is indicated that CeO_x particles near Pt metal have partially oxidized shells that are different from the fully oxidized cores, CeO_2. According to the analysis of Pt, it is confirmed that the $4f_{7/2}$ peak at 72.2 eV is due to the presence of Pt-O_{ads} that could be easily changed to Pt metal under a reductive atmosphere similar to the ORR condition [22]. From the results of TEM and XPS, it is speculated that CeO_x particle combined with PtCo exists as a CeO_2 crystal for the core part and Ce_2O_3 for the shell part.

We examined the electrochemical properties of Pt and PtCo when combined with CeO_x. The electrochemical surface areas (ESAs) evaluated by cyclic voltammetry and the ORR mass activities measured at 0.8 V are summarized in Table 1. PtCo shows higher values of both ESA and ORR mass activity than Pt as reported by other workers [7]. The higher ORR mass activity of PtCo can be partially attributed to the enhancement of the ESA by alloying with Co, but there is no significant change in ESA on the addition of CeO_x to Pt or PtCo. The amount of CeO_x should be selected carefully to achieve the best electrochemical properties because CeO_x is not a good electrical conductor as mentioned before. An excessive addition of CeO_x to Pt or PtCo rather reduces the ESA of catalysts. To determine the optimum CeO_x content, the weight % of Ce is varied from 0 to 12 with paying attention to the effect of Ce content

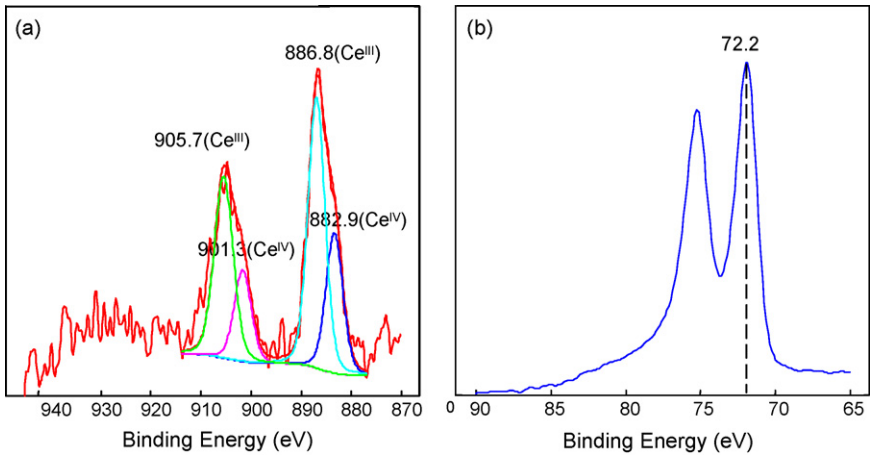

Fig. 3. X-ray photoelectron spectroscopy (XPS) spectra of the (a) Ce 3d and (b) Pt 4f binding energy regions for PtCo–CeO_x/C.

on the onset ORR potential and the limiting current. Although the incorporation of 12 wt.% of Ce has the advantage of increasing the limiting current, the ORR mass activity at 0.8 V is lower than that of Pt or PtCo due to the sacrifice of the onset ORR potential with the addition of Ce. It is found that there is a trade-off between the onset ORR potential and the limiting current in the above Ce content range. The kinetics of the ORR with the optimum CeO_x amount of around 6 wt.% is investigated by using the kinetic current i_k in Fig. 4. The kinetic current is usually expressed by

$$\frac{1}{i} = \frac{1}{i_k} + \frac{1}{i_{lim}} \quad (1)$$

where i is the measured current and i_{lim} is the limiting current. The enhanced ORR kinetics of PtCo–CeO_x compared with PtCo over the potential range from 0.7 to 1.0 V is measured.

Koutecky–Levich plots were obtained over the potential range between 0.7 and 0.8 V, and there exists a linear relationship between the inverse of current and the inverse of the square root of the rotation speed. The linear relationship reported by Lim et al. [27] for ceria-containing electrocatalysts indicates the ORR to have first-order kinetics. Generally, the ORR current is determined by the electrode surface area, the kinematic viscosity of electrolyte, and the concentration and diffusion coefficient of the reactant. Since PtCo and PtCo–CeO_x have similar ESAs and the properties relevant to the electrolyte are unlikely to be different for both catalysts, the increase in the ORR current of PtCo–CeO_x at the above potential range can be attributed to enhanced transport properties of oxygen such as concentration and diffusion coefficient.

An MEA was prepared using the PtCo–CeO_x/C catalyst with the optimum CeO_x amount. A comparison of its performance with

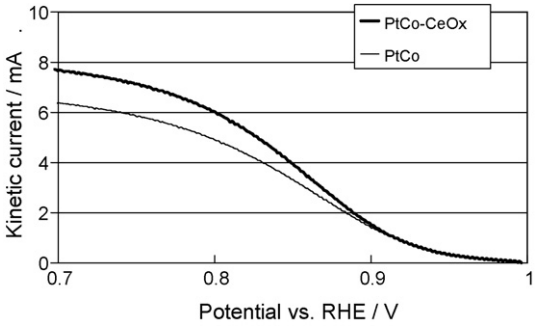

Fig. 4. Oxygen reduction reaction kinetic current of PtCo–CeO_x/C and PtCo/C (rotation speed: 1000 rpm).

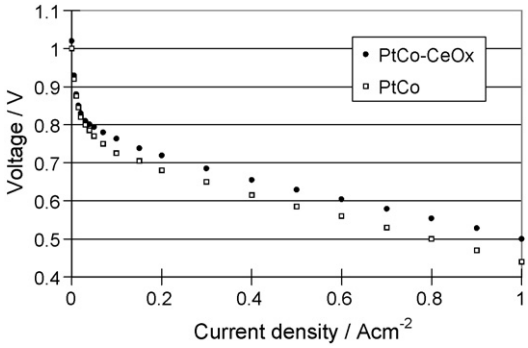

Fig. 5. Performance of MEAs with PtCo–CeO_x/C cathode and PtCo/C cathode.

a MEA using PtCo/C is shown in Fig. 5. The PtCo–CeO_x/C catalyst produces an effect of increased voltage across the entire operating current region compared with PtCo/C, as well as a kinetics-controlled region of less than 0.1 A cm^{-2}. In short, the addition of an optimum amount of CeO_x to PtCo way guarantee a better fuel cell performance than PtCo without CeO_x.

4. Conclusions

Highly dispersed PtCo–CeO_x couples of fine Pt_3Co alloy particles with adjacent CeO_x are synthesized on carbon using the modified colloid method. The average sizes of Pt_3Co and CeO_x particles are approximately 1.7 and 4 nm, respectively. According to XPS studies, the CeO_x particle consists of a CeO_2 phase crystal for the core and a Ce_2O_3 phase for the shell. It seems that the unsaturated Ce_2O_3 phase of CeO_x surface causes the facile adsorption and desorption of oxygen, which leads to an enhanced oxygen supply to the PtCo alloy. The CeO_x-containing samples of PtCo–CeO_x and Pt–CeO_x show improved electrochemical performance for the ORR compared with those without CeO_x in both RDE and cell tests. An optimum cerium content is also suggested on the basis of catalytic mass activity. Further investigations of the preparation method of homogeneous couples between CeO_x and PtCo alloy are required to maximize the ORR activity.

References

[1] R. O'Hayre, S.-W. Cha, W. Colella, F.B. Prinz, Fuel Cell Fundamentals, John Wiley & Sons, New York, 2006, pp. 3–21.
[2] E. Antolini, J.R.C. Salgado, M.J. Giz, E.R. Gonzalez, Int. J. Hydrogen Energy 30 (2005) 1213–1220.

[3] L. Xiong, A.M. Kannan, A. Manthiram, Electrochem. Commun. 4 (2002) 898–903.
[4] M.-K. Min, J. Cho, K. Cho, H. Kim, Electrochim. Acta 45 (2000) 4211–4217.
[5] E. Antolini, R.R. Passos, E.A. Ticianelli, Electrochim. Acta 48 (2002) 263–270.
[6] H. Yano, M. Kataoka, H. Yamashita, H. Uchida, M. Watanabe, Langmuir 23 (2007) 6438–6445.
[7] H.A. Gasteiger, S.S. Kocha, B. Sompalli, F.T. Wagner, Appl. Catal. B: Environ. 56 (2005) 9–35.
[8] V.R. Stamenkovic, B.S. Mun, M. Arenz, K.J.J. Mayrhofer, C.A. Lucas, G. Wang, P.N. Ross, N.M. Markovic, Nat. Mater. 6 (2007) 241–247.
[9] T. Ioroi, T. Akita, S. Yamazaki, Z. Siroma, N. Fujiwara, K. Yasuda, Electrochim. Acta 52 (2006) 491–498.
[10] E. Antolini, J. Power Sources 170 (2007) 1–12.
[11] A.E. Nelson, K.H. Schulz, Appl. Surf. Sci. 210 (2003) 206–221.
[12] H. Yahiro, Y. Bada, K. Eguchi, H. Arai, J. Electrochem. Soc. 135 (1988) 2077–2080.
[13] C.L. Campos, C. Roldan, M. Aponte, Y. Ishikawa, C.R. Cabrera, J. Electroanal. Chem. 581 (2005) 206–215.
[14] J.W. Guo, T.S. Zhao, J. Prabhuram, R. Chen, C.W. Wong, J. Power Sources 156 (2006) 345–354.
[15] J. Wang, J. Xi, Y. Bai, Y. Shen, J. Sun, L. Chen, W. Zhu, X. Qiu, J. Power Sources 164 (2007) 555–560.
[16] J. Wang, X. Deng, J. Xi, L. Chen, W. Zhu, X. Qiu, J. Power Sources 170 (2007) 297–302.
[17] J. Xi, J. Wang, L. Yu, X. Qiu, L. Chen, Chem. Commun. (2007) 1656–1658.
[18] C. Xu, P.K. Shen, Y. Liu, J. Power Sources 164 (2007) 527–531.
[19] H.B. Yu, J.-H. Kim, H.-I. Lee, M.A. Scibioh, J. Lee, J. Han, S.P. Yoon, H.Y. Ha, J. Power Sources 140 (2005) 59–65.
[20] H. Xu, X. Hou, Int. J. Hydrogen Energy 32 (2007) 4397–4401.
[21] S. Koh, J. Leisch, M.F. Toney, P. Strasser, J. Phys. Chem. C 111 (2007) 3744–3752.
[22] M. Watanabe, M. Uchida, S. Motoo, J. Electroanal. Chem. 229 (1987) 395–406.
[23] T.J. Schmidt, H.A. Gasteiger, G.D. Stab, P.M. Urban, D.M. Kolb, R.J. Behm, J. Electrochem. Soc. 145 (1998) 2354–2358.
[24] S. Choi, W. Jeon, H. Sun, D. Lee, D. Seung, H. Ishida, Proceedings of the 210th Meeting Abstract of the Electrochemical Society, vol. 602, 2006, p. 488.
[25] C. Tang, Y. Bando, B. Liu, D. Golberg, Adv. Mater. 17 (2005) 3005–3009.
[26] E.J. Preisler, O.J. Marsh, R.A. Beach, T.C. McGill, J. Vac. Sci. Technol. B 19 (2001) 1611–1618.
[27] D.-H. Lim, W.-D. Lee, D.-H. Choi, H.-H. Kwon, H.-I. Lee, Electrochem. Commun. 10 (2008) 592–596.